Electronic Supplementary Material (ESI) for Chemical Science.

Supporting Information

Quo vadis niobium? Divergent coordination behavior of early-transition metals towards MOF-5

Maciej D. Korzyński, Luca Braglia, Elisa Borfecchia, Kirill A. Lomachenko, Amgalanbaatar Baldansuren, Christopher H. Hendon, Carlo Lamberti and Mircea Dincă*

Table of Contents

Experimental procedures:

Dichloromethane (ACS, >99%, stabilized with amylene), acetonitrile (HPLC Plus, >99.9%), toluene (ACS grade, >99.5%), $Zn(NO_3)_2 \cdot 6H_2O$ (purum p.a., crystallized, >99.0%) and potassium metal (ingot, 99.95%) were purchased from Sigma Aldrich. *N,N*-Dimethylformamide (anhydrous, 99.8%, used for MOF-5 preparation), $(n\text{-}C_4H_9)_3SnH$ (97%, stabilized), chlorotrimethylsilane (98%), 2,3,5,6-tetramethylpyrazine (98%) and terephthalic acid (98+%) were obtained from Alfa Aesar. $NbCl_5$ (99+% Nb), NbO_2 (99+% Nb) and XeF_2 (99.5%) were obtained from Strem. *N*,*N*-Dimethylformamide (HPLC grade, used for washing of MOF-5) and tetrahydrofuran (99.9% min.) were purchased from EMD Millipore. Deionized water was provided via the in-house MIT system. $Zn(NO_3)_2 \cdot 6H_2O$ was kept under dynamic vacuum before MOF-5 synthesis until a free-flowing powder was obtained. *N,N*-Dimethylformamide (DMF), tetrahydrofuran (THF), dichloromethane (DCM), toluene and acetonitrile (MeCN) were dried using a Glass Contour Solvent Purification System, degassed via three freeze-pump-thaw cycles and stored over 4 Å MS in a nitrogen-filled glovebox. $NbCl_4(THF)_2$ complex was obtained from Sigma Aldrich or prepared according to the literature procedure.[1] 2,3,5,6-Tetramethyl-1,4-bis(trimethylsilyl)-1,4-diaza-2,5-cyclohexadiene[2] ($(TMS)_2$pyr), and MOF-5[3] were prepared according to published procedures. Unless otherwise noted, all manipulations were performed in a custom designed MBraun UnilabPro glovebox system under dinitrogen atmosphere (<0.1 ppm of H_2O and O_2). The activated samples were stored in the LC Technology LC-150 glovebox system under argon atmosphere (<0.1 ppm of H_2O and O_2).

Powder X-ray diffraction (PXRD) patterns were recorded on a Bruker Advance II diffractometer equipped with θ/2θ Bragg-Brentano geometry and Ni-filtered Cu-Kα radiation (Kα1 = 1.5406 Å, Kα2 = 1.5444 Å, Kα1/ Kα2 = 0.5). The tube voltage and current were 40 kV and 40 mA, respectively. The data was collected from 3° to 50° of 2θ with a rate of 3 °/minute. A thin, flat layer of sample was placed on the zero background silicon crystal wafer mounted in the sample holder. All measurements were performed with exclusion of moisture and oxygen utilizing an air-free dome setup.

Nitrogen adsorption isotherms were measured using a Micromeritics ASAP 2020 Plus Surface Area and Porosity Analyzer. In a typical measurement, an oven-dried sample tube was brought into the argon filled glovebox and its weight was recorded five times. The tube was filled with approximately 35 mg of the desired activated material and the weight was measured five times again. The mass of the sample was obtained from subtraction of the averaged masses before and after the sample was placed in the tube. The tube was capped with a S3 TranSeal™ (Micromeritics), brought out of the glovebox, and transferred to the analysis port of the gas sorption analyzer. The samples were heated at 150 °C under vacuum prior to measurements until the outgas rate was less than 2 mtorr/minute. N_2 isotherms were measured using liquid nitrogen baths (77 K). UHP grade (99.999% purity, Airgas) N_2 and He, oil-free valves and gas regulators were used for all free space corrections and measurements. The Brunauer–Emmett–Teller (BET) surface areas (SA) were obtained from the software supplied with the instrument; BET consistency criteria were met for all of the samples.[4]

Inductively coupled plasma – atomic emission spectroscopy (ICP-AES) analysis of niobium and zinc content was performed using Agilent 5100 DVD Inductively Coupled Plasma-Optical Emission Spectrometer equipped with argon humidifier operating in radial detection mode. For each element two spectral lines were observed: 202.548, **213.857** nm for Zn and **309.417**, 313.078 nm for Nb (bolded used for calculations). Calibration curves were obtained by dilution of the commercially available standard solutions (Ricca Chemical Company). A typical MOF sample of ca. 10 mg was weighed out in the argon filled glovebox. The sample was treated overnight with 50 μL of concentrated HF (EMD Millipore, 47-51%, Omnitrace) and 950 μL of concentrated nitric acid (EMD Millipore, 67-70%, Omnitrace). The samples were diluted using 19 mL of reverse osmosis water to yield solutions in the 0-200 ppm range (within the calibration curve). The remaining organic residue was separated by centrifugation.

Attenuated total reflection Fourier-transform infrared (ATR-FTIR) spectroscopy was performed using Bruker ALPHA II Spectrometer (MIR source and KBr beam splitter) equipped with RT-DLaTGS detector

utilizing Platinum ATR accessory. The data was averaged over 32 scans between 4000 - 400 cm^{-1} (4 cm^{-1} resolution). The measurements were performed in a nitrogen-filled glovebox.

Field Emission Scanning Electron Microscopy (FESEM) was performed using Zeiss Supra55VP Microscope. A small amount of sample was dispersed on the carbon tape attached to an aluminum stub in an argon-filled glovebox. Prior to measurements the samples were coated with a layer of carbon. FESEM data was obtained at beam voltage of 15 kV and working distance of 8.5 mm with an Everhart-Thornley (SE2) detector. Elemental mapping was realized using an energy dispersive X-ray spectrometer (EDX) integrated with the FESEM instrument. A dwell time of 200 µs was used to collect 1024 x 800 px EDX maps.

X-ray absorption spectroscopy (XAS) experiments were performed at the BM23 beamline of the European Synchrotron Radiation Facility (ESRF, Grenoble, France).[5] We worked in transmission mode at the Nb K-edge (18990 eV), using the Si(111) double-crystal monochromator to monocromatize the X-ray beam, while the harmonic rejection was performed by using two silicon mirrors at a 4 mrad angle. Spectra were collected using 30 cm ionization chambers for measuring the incident beam (I_0), the beam transmitted through the sample, and the reference (I_1 and I_2 respectively). The weights of the pellets were optimized to obtain the best signal/noise ratio for XAS measurements in transmission mode ($\Delta\mu x \approx 0.3$ with estimated total absorption of ≈ 1.8), resulting in 77.5 mg per 1.3 cm^2 pellets. The XAS data reduction and EXAFS extraction procedure were performed using the Athena code.[6] Once extracted, the k^3-weighted $\chi(k)$ functions were Fourier-transformed in a Δk range ($\Delta k = 3.2 – 13$ $Å^{-1}$) and fitted in R-space in the $\Delta R = 1.0 – 4$ Å range, potentially resulting in 20 independent parameters ($2\Delta k \Delta R/\pi > 20$). Athena software was used to normalize the data while Artemis software was employed for the EXAFS analysis. Phases and amplitudes were calculated by the FEFF6 code, implemented in the Artemis software from the Demeter package,[6] using the DFT-optimized structure of Nb-MOF-5. The parameters optimized in the EXAFS fit for Nb-MOF-5 sample are reported in the Table S2 and S3. The parameterization of the EXAFS paths was performed including all the first shell single scattering (SS) paths with specific ΔR and Debye-Waller (σ^2) parameters

of Cl, O and Zn atoms. For remaining atoms located at a distance larger than 3.3 Å from the absorber, the SS paths and the rather intense, multiple scattering (MS) paths were included in the fitting model with an isotropic parametrization strategy. These paths were modeled considering global isotropic contraction/expansion factor for the whole MOF framework α and a σ^2 increasing as the square root of the distance $R_{eff,i}$ of the i^{th} scattering atom from the absorber ($\Delta R_{framework,i} = \alpha R_{eff,i}$; $\sigma^2_i = \sigma^2 (R_{eff,i}/R_{short})^{1/2}$ where R_{short} refers to the shortest path of this group, resulting in only two optimized parameters: α, σ^2), as already successfully employed in previous EXAFS analyses. A variety of Nb reference samples were used to support the EXAFS parameterizations.

Continuous wave electron paramagnetic resonance (CW EPR) measurements were performed on a Bruker ElexSys E500 spectrometer fitted with a finger dewar. The data was collected at 77 K using J. Young EPR tubes to exclude air and moisture, as suspensions in THF (dry and degassed). Microwave powers ranging from 0.6325 to 2 mW were applied. EasySpin[7], a MATLAB simulation toolbox was used, particularly for obtaining a principal parameter set of effective g-values and hyperfine interactions of ^{93}Nb with I = 9/2. In the numerical spectrum simulations of continuous wave EPR spectra of Nb(IV)-MOF-5, high-field approximations, $\beta_e \mathbf{B_0} \cdot \mathbf{g} \cdot \mathbf{S} >> h\mathbf{S} \cdot \mathbf{A} \cdot \mathbf{I}$, were assumed so that the effects of the nuclear field on the alignment of the electron spin is negligible, thus the electron problem is treated independently. Hyperfine interaction is treated as the perturbation of the electron Zeeman level. The corresponding energy levels are well-separated and m_S becomes a main quantum number. The coaxial orientation of g and A is assumed for the simulations. It does not use perturbation theory, and each nucleus is treated independently allowing arbitrary magnitudes and orientations of the hyperfine matrices of the near equivalent nuclei. Powder EPR spectra were evaluated considering a large set of different orientations of paramagnetic centers uniformly distributed over the unit sphere. The simulated spectra were further fitted to the experimental spectra using the least-squares fitting algorithms, implemented in EasySpin[7]. The Voigtian broadening function, considering unresolved hyperfine interactions, deviates slightly from a pure Lorentzian function since the FWHM also has a contribution from a Gaussian component.

Solvent selection for the deposition of Nb(IV) species. THF, DMF and MeCN were initially considered as a solvent of choice for immobilization of $NbCl_4(THF)_2$. THF was unsuitable for the process due to the low solubility of the complex. Additionally, a survey soak using 40 equivalents of the niobium precursor per SBU in DMF led to dissolution of the MOF-5 crystals. Consequently, MeCN was chosen as the solvent for the niobium incorporation.

Preparation of Nb(IV)-MOF-5, general method. Activated MOF-5 (200 mg, 0.26 mmol) was pretreated with 2 mL of MeCN. The desired amount of $NbCl_4(THF)_2$ (0.17 eq for 0.16 mol_{Nb} per SBU, 0.25 eq for 0.20 mol_{Nb} per SBU, 0.5 eq for 0.52 mol_{Nb} per SBU, 1 eq for 1.12 mol_{Nb} per SBU) was dissolved in a volume of MeCN yielding 5 mM solution of the precursor. MOF-5 crystals were added in one portion and the resulting mixture was swirled for 5 minutes to prevent crystals from sticking to the walls of the reaction vessel. Almost immediately the colorless MOF crystals started turning dark violet. The mixture was placed on a blot mixer. After 48 hours the soaking solution was decanted, and solids were soaked in fresh MeCN (20 mL, 2 times, 24 hours each) followed by DCM (20 mL, 2 times, 24 hours each). After the last washing step, Nb(IV)-MOF-5 crystals were activated by heating to 150 °C under high vacuum for 24 hours or until 0.1 mTorr was reached.

Treatment of Nb(IV)-MOF-5 with XeF_2. *Experiments involving XeF_2 were performed in plastic vials to avoid etching of the glass*. Nb(IV)-MOF-5 (20 mg) was pretreated with 2 mL of MeCN. XeF_2 (10 mg, 0.06 mmol) was dissolved in 7 mL of MeCN and added to the vial containing the MOF. The mixture was left on a blot mixer for 24 hours. The MOF crystals became off-white and the solution became yellow. The liquid phase was decanted and a fresh solution of XeF_2 (10 mg, 0.06 mmol, in 7 mL of MeCN). The mixture was left on a blot mixer for another 24 hours. The soaking solution was decanted, and solids were soaked in fresh MeCN (10 mL, 4 times, 2 hours each).

Preparation of Nb(V)-MOF-5. Activated MOF-5 (153 mg, 0.20 mmol) was pretreated with 2 mL of MeCN. $NbCl_5$ (27.0 mg, 0.10 mmol) was dissolved in 20 mL of MeCN to yield a yellow solution. MOF crystals were added in one portion and the resulting mixture was swirled for 5 minutes to prevent crystals

from sticking to the walls of the reaction vessel. The mixture was left on a blot mixer. After 48 hours the color of the solution faded and the colorless crystals of MOF-5 became off-white. The soaking solution was decanted, and solids were soaked in fresh MeCN (20 mL, 2 times, 24 hours each).

Reduction of Nb(V)-MOF-5 using $(TMS)_2$pyr. $(TMS)_2$pyr (40 mg, 0.14 mmol) was dissolved in 5 mL of THF. The solution was added in one portion to a vial containing 40 mg of Nb(V)-MOF-5. Almost immediately a change of color to dark blue could be observed. After 30 minutes the solution was decanted, and solids were washed with fresh tetrahydrofuran (10 mL, 3 times, 1 hour each).

Computational details:

Starting with the crystallographic structure of pristine MOF-5, the material was first geometrically optimized within the DFT framework as implemented in VASP.[8] A 500 eV planewave cutoff and the PBEsol[9] functional were used, with the resulting structure being electronically converged to within 0.005 eV per atom and within 2% of the experimental lattice parameters. HSE06,[10] a hybrid functional, was then used to recover more accurate electronic properties, and the resulting electronic band gap was found to be in agreement with experiment. Nb defects and appendages were then made to the optimized periodic structure. Only Schottky defects were considered (i.e. high-valence Nb was explicitly passivated by inner sphere counter anions). Using the same procedure for the initial optimization of the parent material, the Nb-containing frameworks were recovered. In systems that had multiple possible spin orientations all relevant electronic configurations were examined, and the lowest energy configuration was selected as the most plausible candidate.

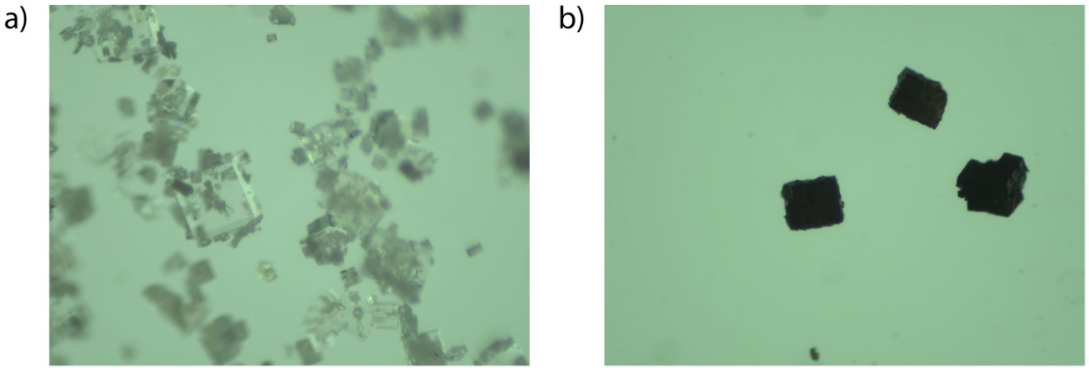

Figure S1. Appearance of the a) MOF-5 and b) Nb(IV)-MOF-5 crystals.

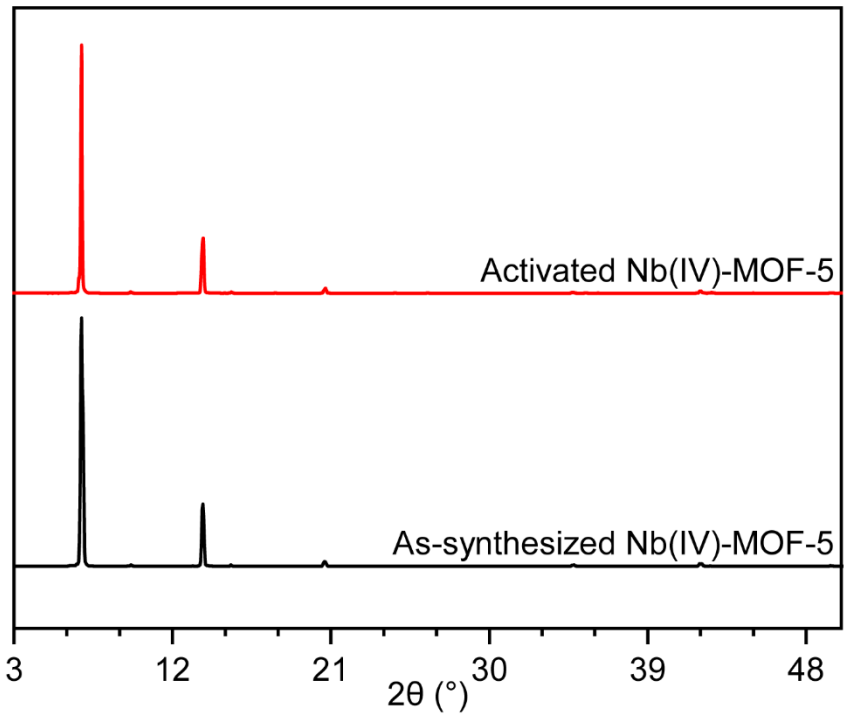

Figure S2. Comparison of PXRD patterns for activated and as-synthesized Nb(IV)-MOF-5.

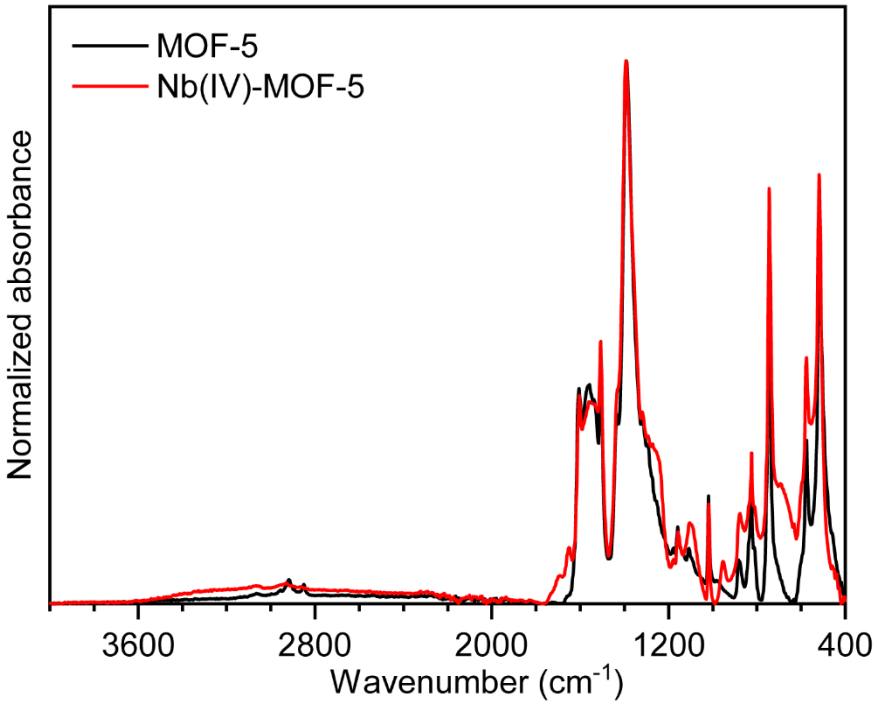

Figure S3. Comparison of ATR-FTIR spectra of MOF-5 and Nb(IV)-MOF-5.

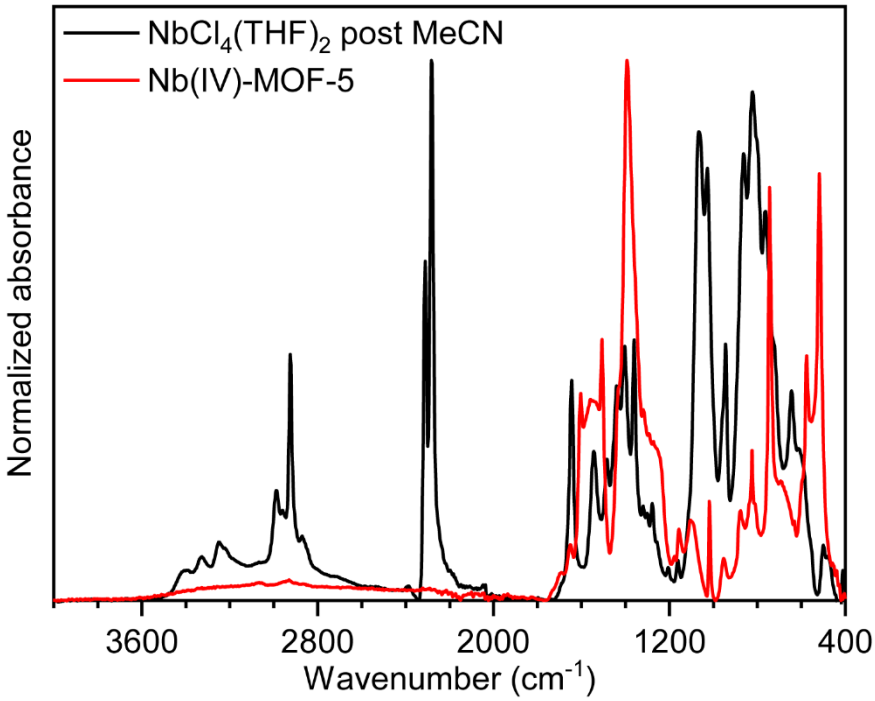

Figure S4. Comparison of ATR-FTIR spectra of MOF-5 and vacuum dried acetonitrile solution of $NbCl_4(THF)_2$.

Table S1. Spin Hamiltonian parameters obtained from least-squares fittings for Nb(IV)-MOF-5.

g_1	g_2	g_3	g_{iso}	A_1 (MHz)	A_2 (MHz)	A_3 (MHz)	A_{iso} (MHz)	Nucleus
1.995	1.960	2.006[a]	1.987	671	538	461	557	^{93}Nb
				-1.01	0.96	173	173	$^{(35,37)}$Cl

[a]A positive deviation from a free electron g_e value is likely due to strain effects, i.e. distribution of spin Hamiltonian parameters: g-strain and unresolved hyperfine splitting.

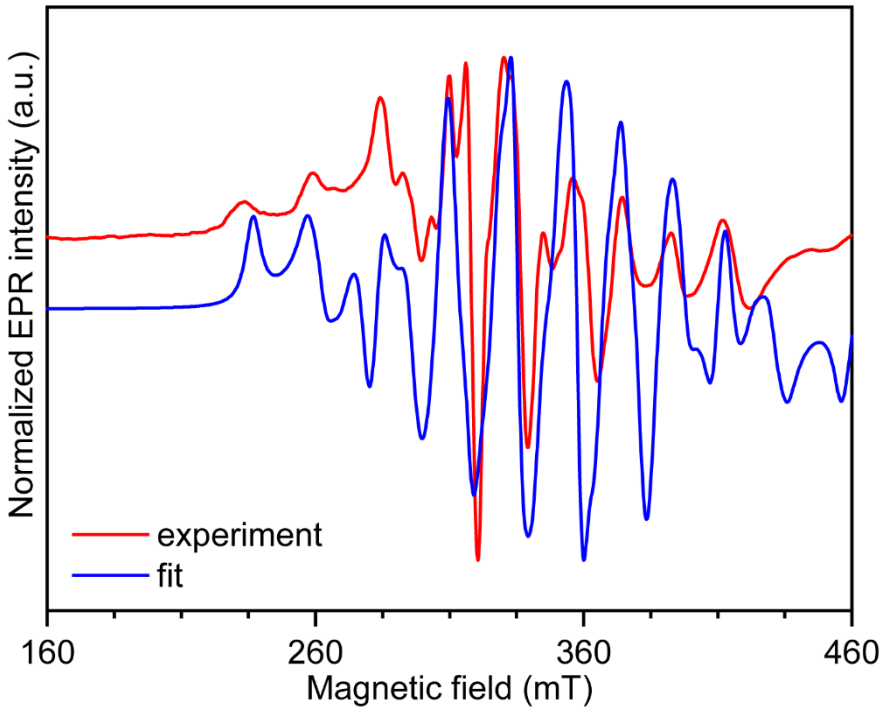

Figure S5. First derivative EPR fit of the Nb(IV)-MOF-5 signal.

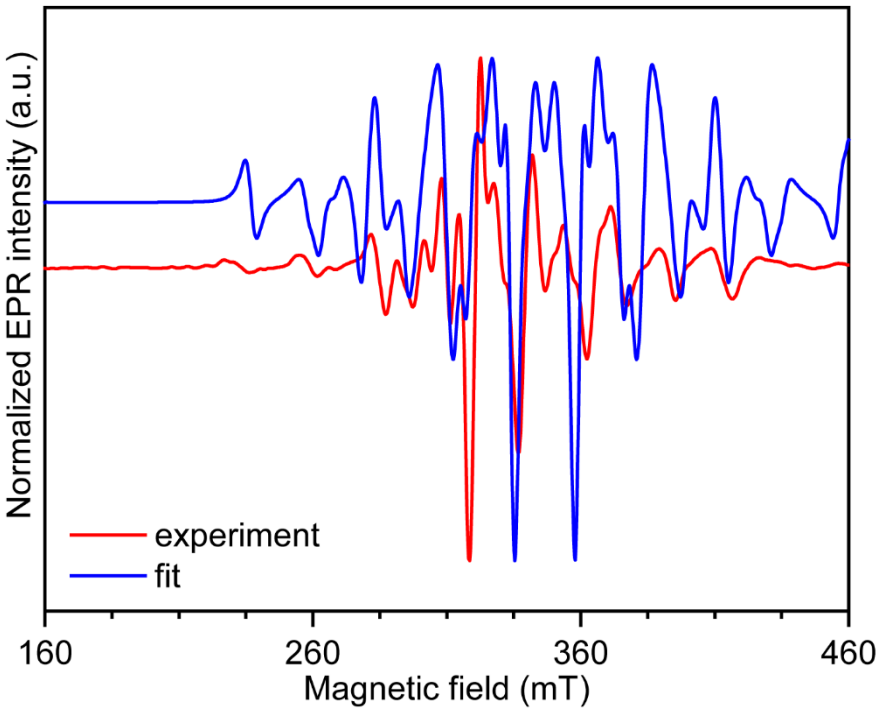

Figure S6. Second derivative EPR fit of the Nb(IV)-MOF-5 signal.

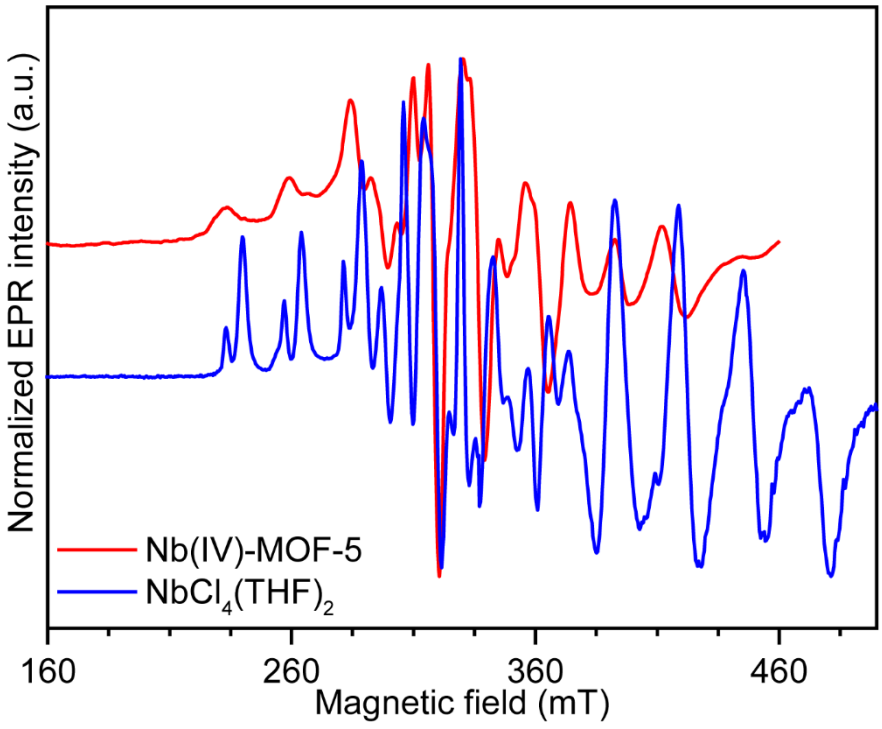

Figure S7. Comparison of the first derivative EPR signal for Nb(IV)-MOF-5 and an acetonitrile/toluene frozen glass of $NbCl_4(THF)_2$.

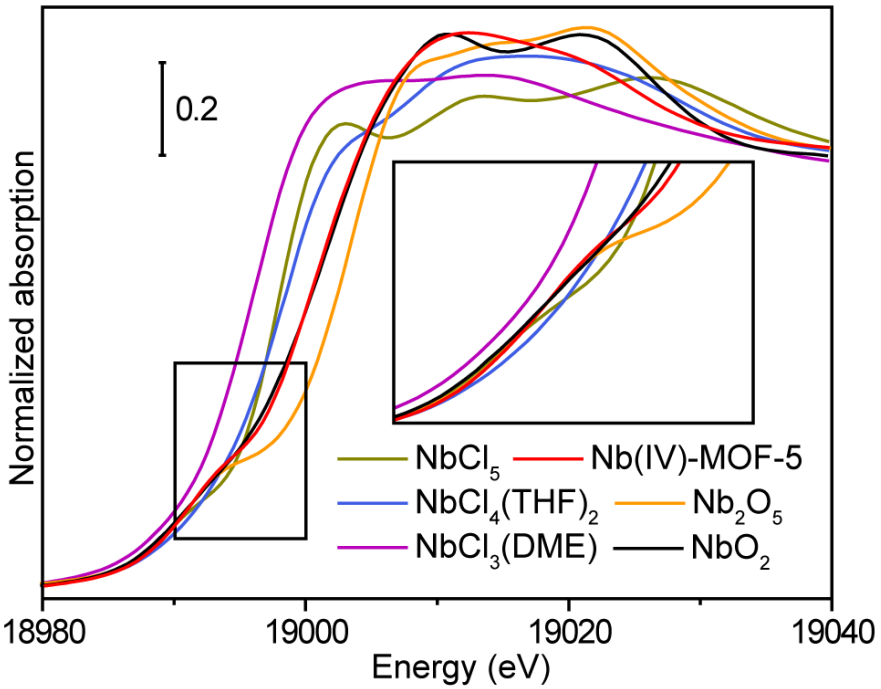

Figure S8. Nb K-edge XANES spectra of Nb(IV)-MOF-5 and selected reference compounds.

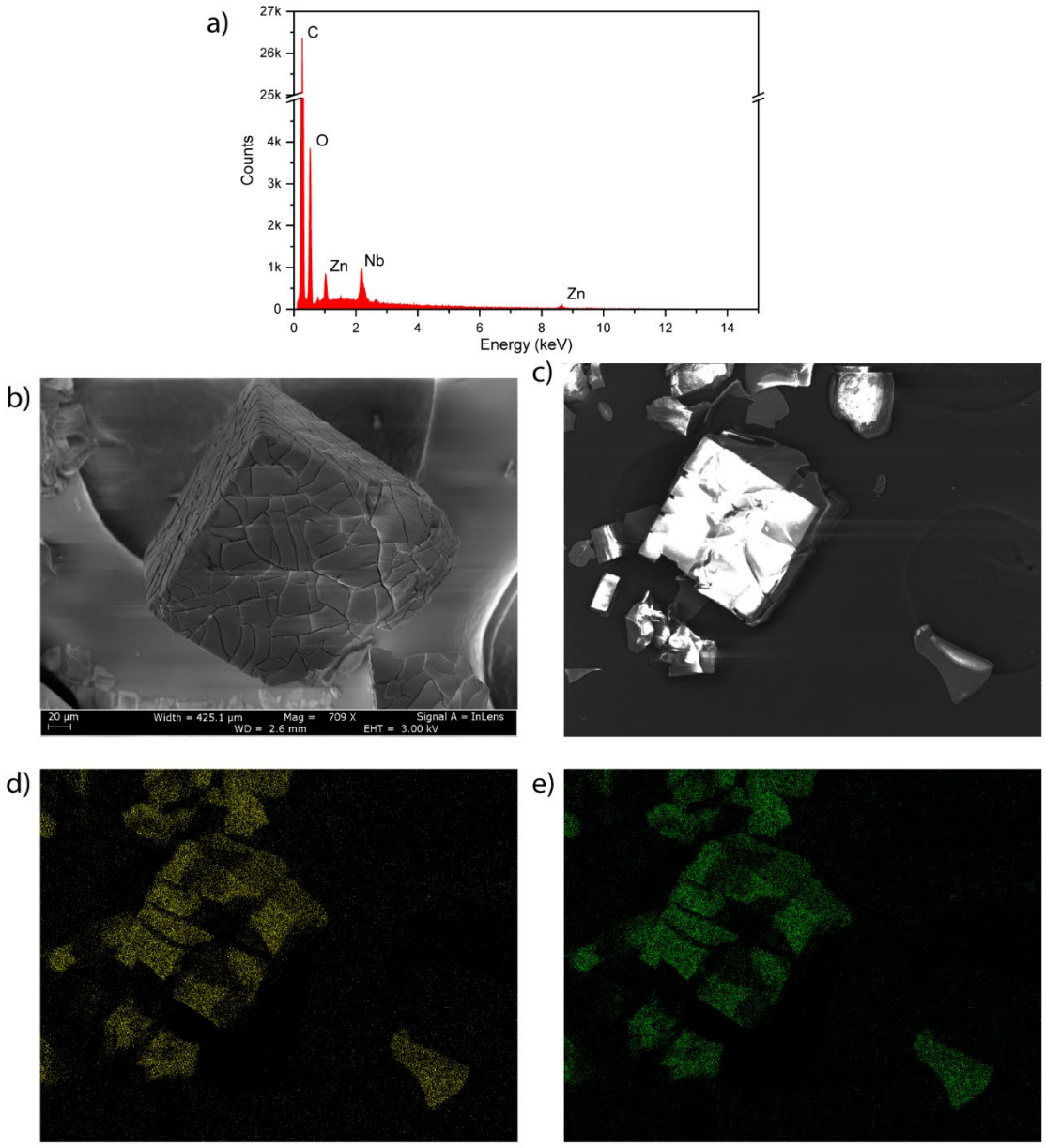

Figure S9. SEM/EDX imaging/mapping of intact Nb(IV)-MOF-5; a) EDX scan of the bulk material, b) SEM image of the material, c) SEM image for EDX mapping, d) Zn L-edge mapping and e) Nb L-edge mapping.

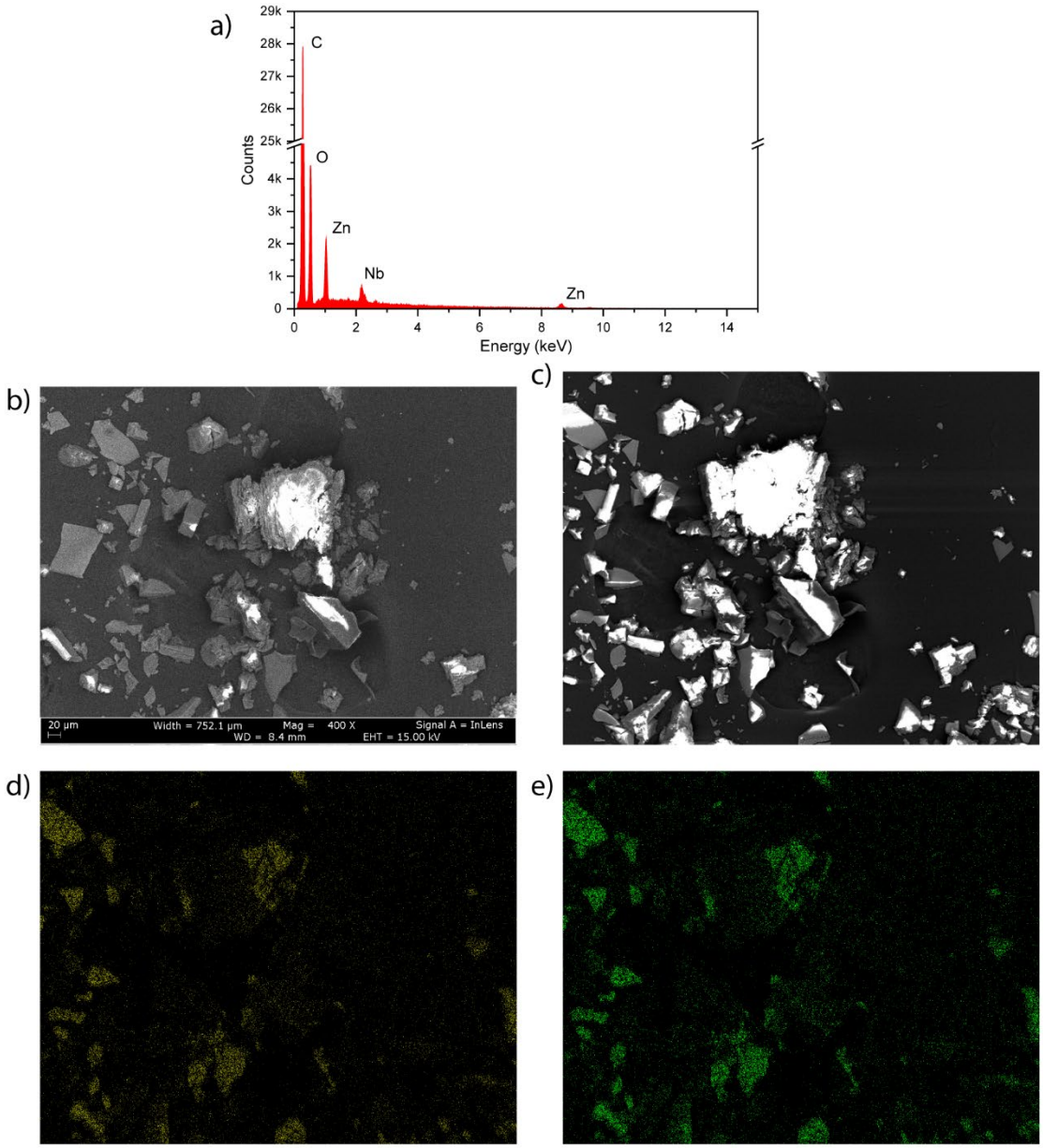

Figure S10. SEM/EDX imaging/mapping of crushed Nb(IV)-MOF-5; a) EDX scan of the bulk material, b) SEM image of the material, c) SEM image for EDX mapping, d) Zn L-edge mapping and e) Nb L-edge mapping.

Table S2. 1st refinement: Best-fit values of the parameters optimized in the EXAFS fits for the three Nb(IV)-MOF-5 binding scenarios under He at RT. The fits were performed in the k-space interval Δk = (3.2–13) $Å^{-1}$ and R-space interval ΔR = (1.0–4.0) Å. A global contraction/expansion factor α was used and σ^2 that increase as the square root of the distance $R_{eff,i}$ of the i^{th} scattering atom from the absorber ($\Delta R_{framework,i} = \alpha R_{eff,i}$; $\sigma^2_i = \sigma^2 (R_{eff,i}/R_{short})^{1/2}$ where R_{short} refers to the shortest path of this group. The underscored values have been fixed in the EXAFS analysis. The values reported in brackets fall suspiciously outside of their respective expected ranges, thus indicating an imperfect fitting model.

EXAFS Fit parameters	**'$NbCl_4$'**	**'$NbOCl_2$'**	**'$NbCl_2$'**
S_0^2	<u>1</u>	<u>1</u>	<u>1</u>
ΔE (eV)	-3 ± 3	(-15 ± 31)	4 ± 4
R-Factor	0.1	(0.5)	(0.7)
$N°_{par}/N°_{ind}$	8/20	8/20	7/20
N_{Cl}	<u>4</u>	<u>2</u>	<u>2</u>
N_O	<u>2</u>	<u>3</u>	<u>4</u>
$<R_O>$ (Å)	2.47 ± 0.03	2.28 ± 0.09	2.07 ± 0.02
$<R_{O1}>$ (Å)	–	1.67 ± 0.1	–
σ_O^2 ($Å^2$)	<u>0.005</u>	<u>0.005</u>	<u>0.005</u>
$<R_{Cl}>$ (Å)	2.25 ± 0.02	2.24 ± 0.1	2.38 ± 0.02
$<R_{Cl1}>$ (Å)	2.41 ± 0.02	–	–
σ_{Cl}^2 ($Å^2$)	<u>0.004</u>	<u>0.004</u>	<u>0.004</u>
R_{Zn} (Å)	3.28 ± 0.01	2.97 ± 0.3	3.53 ± 0.2
σ_{Zn}^2 ($Å^2$)	0.01 ± 0.01	0.01 ± 0.03	0.008 ± 0.016
α	0.05 ± 0.02	-0.02 ± 0.19	0.02 ± 0.04
σ^2 ($Å^2$)	0.01 ± 0.01	(0.14 ± 0.12)	(0.001 ± 0.01)

Table S3. 2nd refinement: Best-fit values of the parameters optimized in the EXAFS fits for the three Nb(IV)-MOF-5 binding scenarios under He at RT. The fits were performed in the k-space interval Δk = (3.2–13) $Å^{-1}$ and R-space interval ΔR = (1.0–4.0) Å. The underscored values have been fixed in the EXAFS analysis. The values reported in brackets fall suspiciously outside of their respective expected ranges, thus indicating an imperfect fitting model. The relatively high value of the obtained R-factors most probably reflects a minor heterogeneity in the Nb environment.

EXAFS Fit parameters	**'$NbCl_4$'**	**'$NbOCl_2$'**	**'$NbCl_2$'**
S_0^2	0.7 ± 0.2	0.8 ± 0.1	(0.51 ± 0.04)
ΔE (eV)	-4 ± 3	0 ± 3	(10 ± 2)
R-Factor	0.07	0.10	0.09
$N°_{par}/N°_{ind}$	9/20	9/20	8/20
N_{Cl}	4	2	2
N_O	2	3	4
$<R_O>$ (Å)	2.49 ± 0.05	2.04 ± 0.02	2.12 ± 0.02
$<R_{OI}>$ (Å)	–	1.75 ± 0.02	–
σ_O^2 ($Å^2$)	0.005	0.005	0.005
$<R_{Cl}>$ (Å)	2.23 ± 0.04	2.33 ± 0.02	2.40 ± 0.02
$<R_{ClI}>$ (Å)	2.38 ± 0.02	–	–
σ_{Cl}^2 ($Å^2$)	0.004	0.004	0.004
R_{Zn} (Å)	3.25 ± 0.06	2.79 ± 0.24	3.73 ± 0.08
σ_{Zn}^2 ($Å^2$)	0.008 ± 0.007	0.03 ± 0.03	0.004 ± 0.009
α	0.04 ± 0.01	0.04 ± 0.03	0.07 ± 0.04
σ^2 ($Å^2$)	0.002 ± 0.006	(0.03 ± 0.13)	(0.002 ± 0.016)

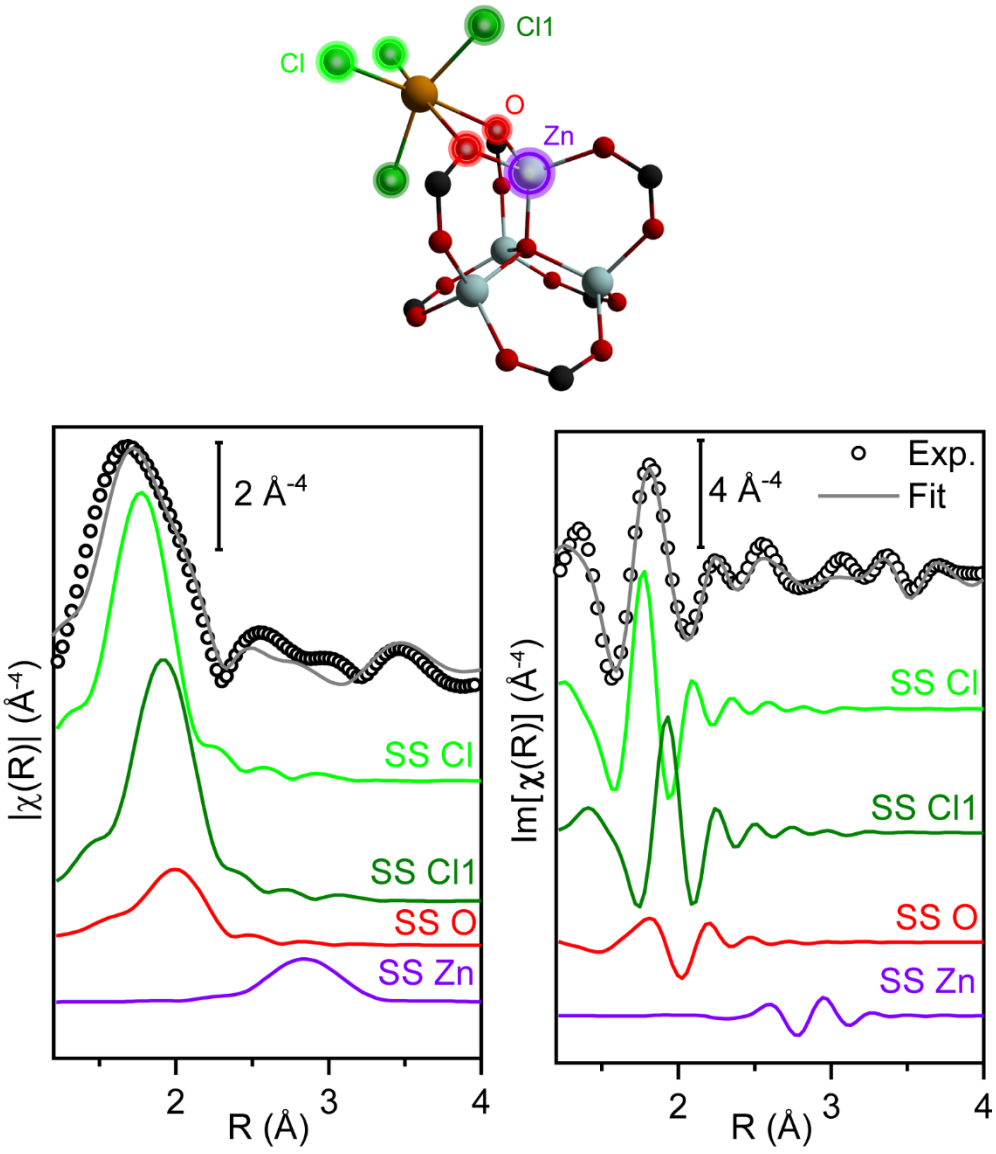

Figure S11. Individual scattering path contributions to the best fit EXAFS model of Nb(IV)-MOF-5.

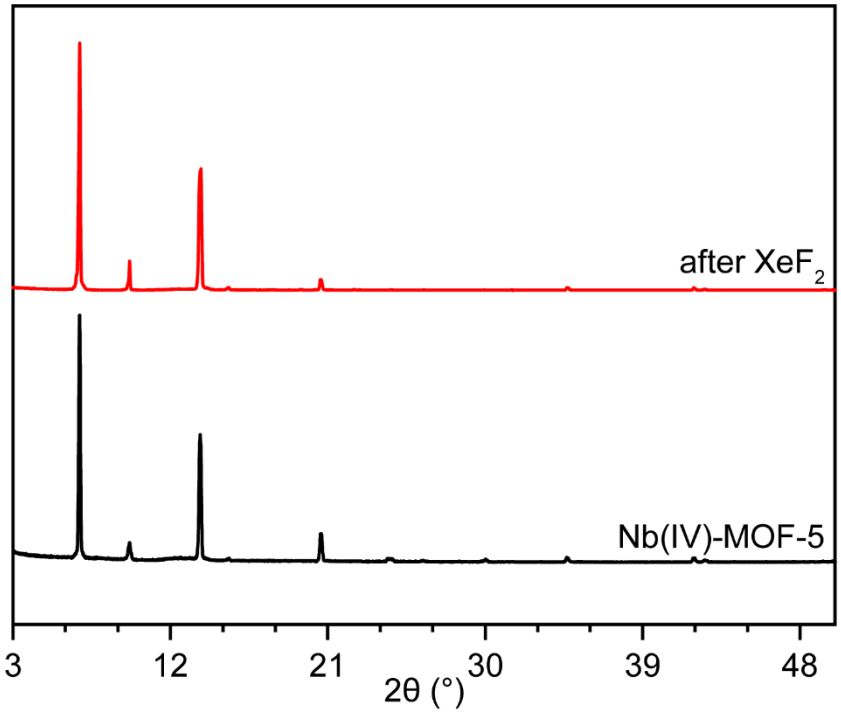

Figure S12. PXRD pattern of Nb(IV)-MOF-5 berfore and after XeF_2 treatment.

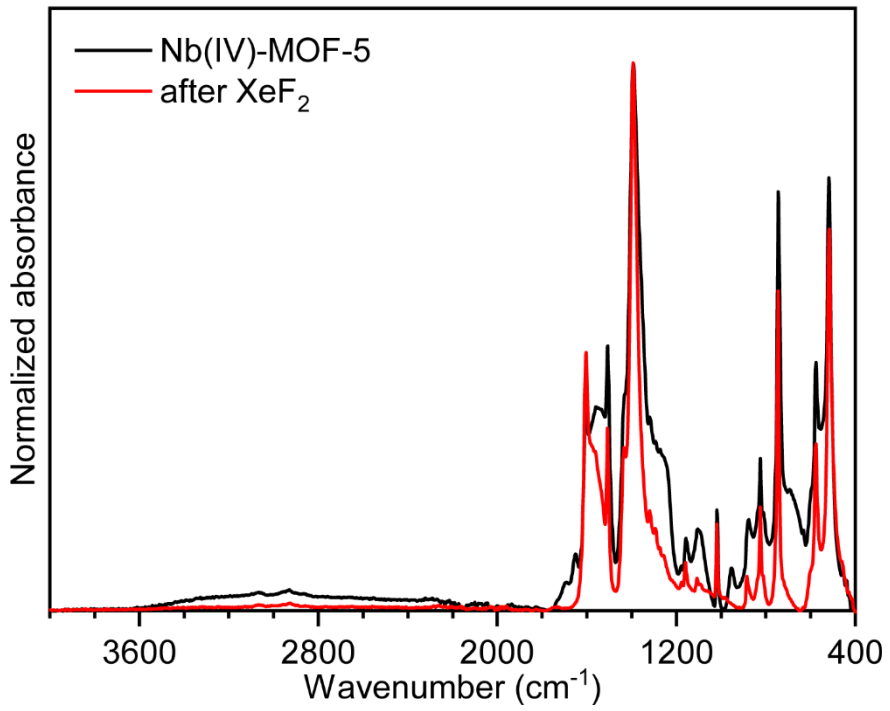

Figure S13. ATR-FTIR spectrum of Nb(IV)-MOF-5 before and after XeF_2 treatment.

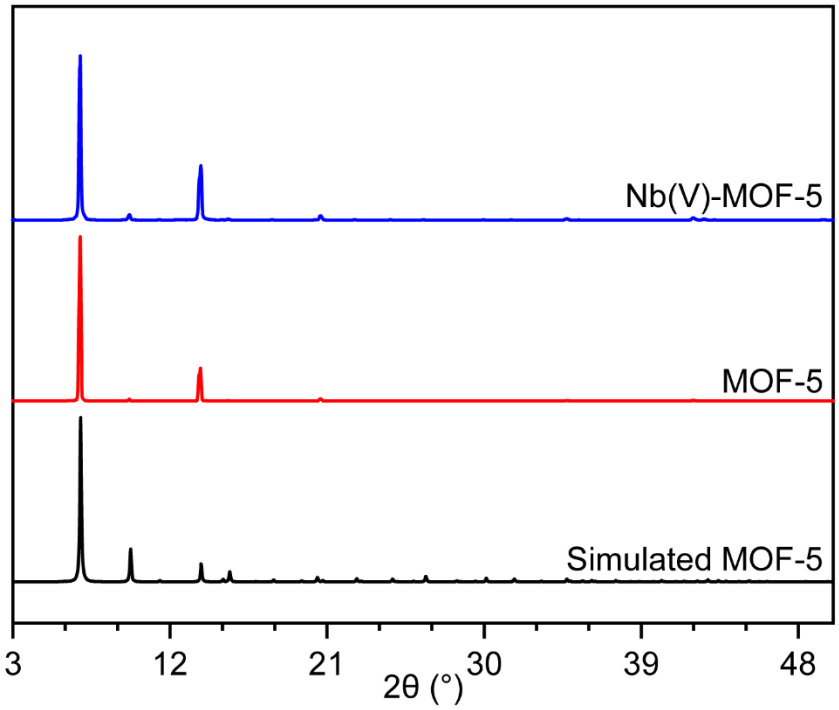

Figure S14. PXRD pattern of the activated Nb(V)-MOF-5.

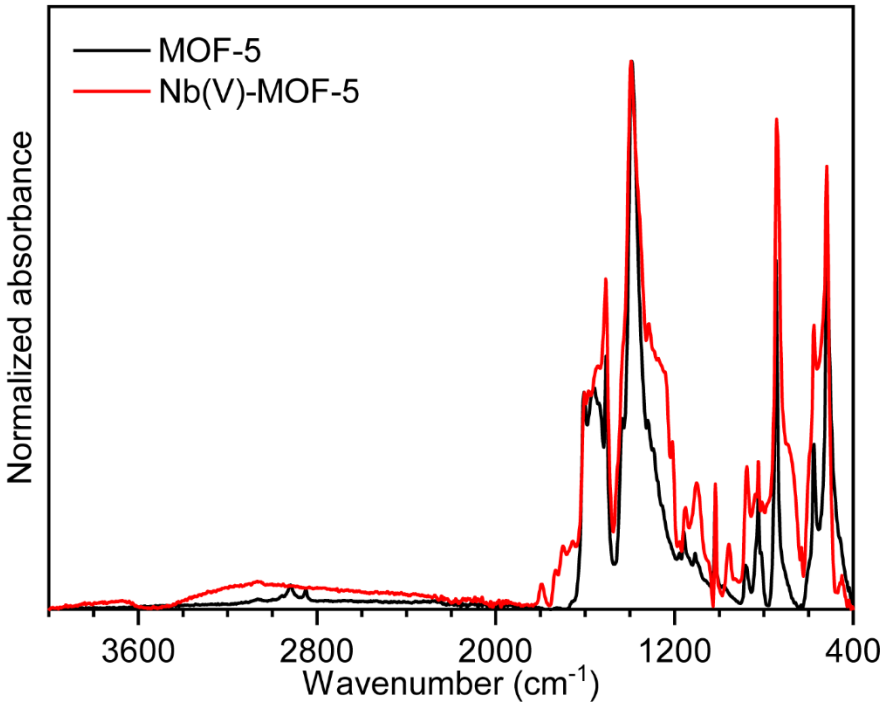

Figure S15. Comparison of ATR-FTIR spectra of MOF-5 and Nb(V)-MOF-5.

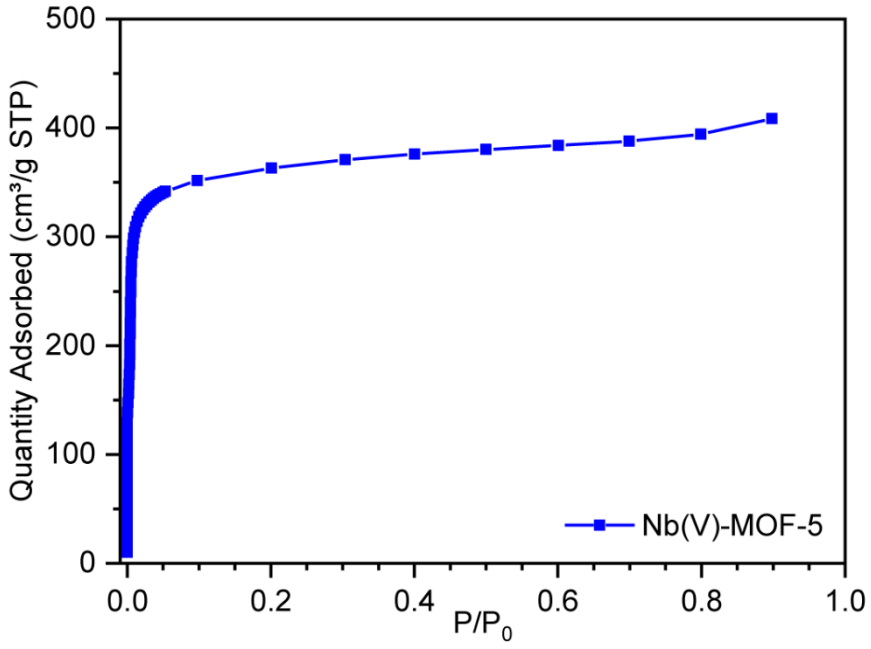

Figure S16. Nitrogen adsorption isotherm of Nb(V)-MOF-5 (BET SA 1437 m^2/g) at 77 K.

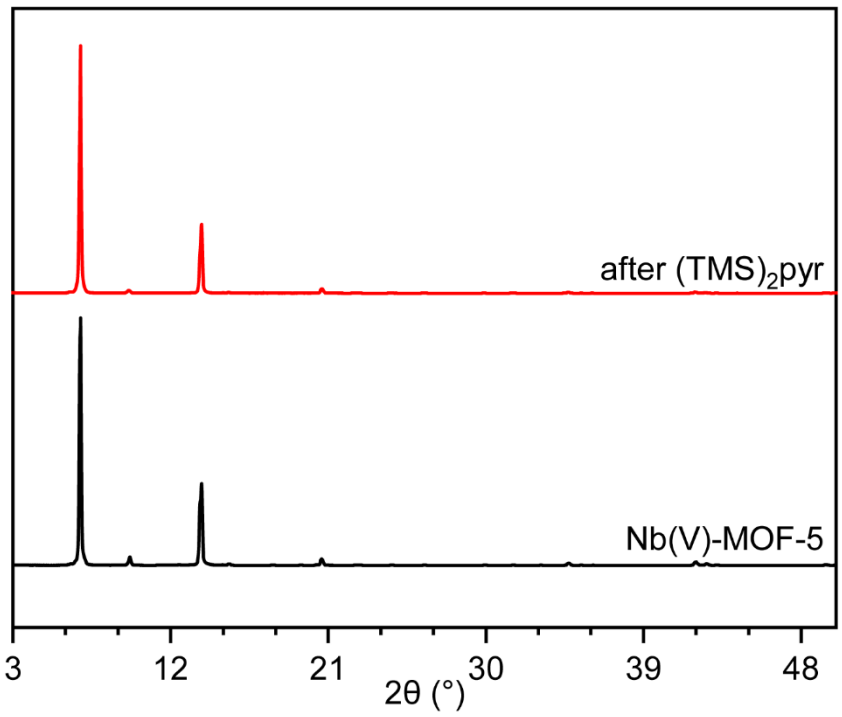

Figure S17. PXRD pattern of Nb(V)-MOF-5 before and after $(TMS)_2$pyr.

References:

1 S. F. Pedersen, J. B. Hartung, E. J. Roskamp, P. S. Dragovich, C. J. Ruffing and B. A. Klein, in *Inorganic Syntheses*, ed. R. N. Grimes, 2007, vol. 29, pp. 119–123.

2 W. Kaim, *J. Am. Chem. Soc.*, 1983, **105**, 707–713.

3 S. S. Kaye, A. Dailly, O. M. Yaghi and J. R. Long, *J. Am. Chem. Soc.*, 2007, **129**, 14176–14177.

4 T. C. Wang, W. Bury, D. A. Gómez-Gualdrón, N. A. Vermeulen, J. E. Mondloch, P. Deria, K. Zhang, P. Z. Moghadam, A. A. Sarjeant, R. Q. Snurr, J. F. Stoddart, J. T. Hupp and O. K. Farha, *J. Am. Chem. Soc.*, 2015, **137**, 3585–3591.

5 O. Mathon, A. Beteva, J. Borrel, D. Bugnazet, S. Gatla, R. Hino, I. Kantor, T. Mairs, M. Munoz, S. Pasternak, F. Perrin and S. Pascarelli, *J. Synchrotron Radiat.*, 2015, **22**, 1548–1554.

6 B. Ravel and M. Newville, *J. Synchrotron Radiat.*, 2005, **12**, 537–541.

7 S. Stoll and A. Schweiger, *J. Magn. Reson.*, 2006, **178**, 42–55.

8 G. Kresse and J. Furthmüller, *Phys. Rev. B*, 1996, **54**, 11169–11186.

9 J. P. Perdew, K. Burke and M. Ernzerhof, *Phys. Rev. Lett.*, 1996, **77**, 3865–3868.

10 J. Heyd, G. E. Scuseria and M. Ernzerhof, *J. Chem. Phys.*, 2006, **124**, 219906.

Author Contributions:

MDK and MD conceptualized the project. MDK performed the synthetic work, reactivity studies and characterization of the materials. LB, EB, KAL collected and analyzed the XAS data under the supervision of CL. AB analyzed the EPR data. CHH performed the DFT calculations. MDK and MD wrote the manuscript with input from all of the authors.